Semnan University

Journal of Modeling & Simulation in Electrical & Electronics Engineering (MSEEE)

Journal homepage: https://mseee.semnan.ac.ir/

ISSN: 2821-0786

Economic Assessment and Optimal Sizing of Energy and Storage Systems of a Grid-Connected Turbo-Expander Based Microgrid with Simultaneous Recovery of Cooling and Electrical Energy at Natural Gas Pressure Reduction Stations

Reza Ghanaee[1] and Asghar Akbari Foroud[1]*

***Abstract*-- This paper proposes a novel microgrid configuration integrated with a turbo-expander (TE), in which the recovered cooling and electrical energy are utilized to supply part or all of the microgrid demand. The proposed grid-connected microgrid is designed to optimally select the type and capacity of energy generation and storage systems over a 20-year planning horizon. A multi-objective optimization framework based on the Particle Swarm Optimization (PSO) algorithm is employed to minimize the annualized capital investment as well as operation and maintenance (O&M) costs. The microgrid comprises an internal combustion engine (ICE), photovoltaic (PV) system, battery bank (BB), auxiliary boiler (AB), heat storage tank (HST), absorption chiller (AC), and electric chiller (EC) to meet the electrical, heating, and cooling demands. A comparative economic analysis is performed for two optimal configurations, with and without the TE. The results demonstrate that the TE-based microgrid reduces O&M and emission costs by approximately 34% and 35.2%, respectively, compared with the conventional microgrid. Moreover, cash flow analysis verifies the economic feasibility of the proposed TE-based microgrid.**

***Index Terms:* Turbo-Expander, Exergy, Microgrid, Optimal sizing problem, Cash flow analysis.**

I. Introduction

According to the Paris Agreement, the increase in global average temperature should be limited to below 2 °C by 2100 [1]. One of the primary approaches to achieving this target is reducing the use of highly polluting fossil fuels, such as coal, and replacing them with natural gas (NG). Raw NG extracted from wells, after liquid removal and processing, is delivered to consumers mainly through two methods: transmission pipelines and liquefied natural gas (LNG) transportation [2]. In pipeline transmission systems, NG is compressed at compressor stations and transported at high pressure to consumption centers. However, in end-use locations such as refineries, power plants, and urban areas, the delivered pressure is unsuitable for direct utilization and must be reduced in pressure regulating stations (PRSs) according to consumer requirements. In conventional PRSs, pressure regulators are employed to adjust the NG pressure. This pressure reduction is an isenthalpic expansion process that results in exergy loss, which is dissipated as heat. In contrast, a TE enables secure pressure reduction while

Submit Date; 2025-12-30 Revise Date; 2026-07-27 Accept Date; 2026-08-17

1. Electrical and Computer Engineering Faculty, Semnan University, Semnan, Iran.
Correspondence: aakbari@semnan.ac.ir

Cite this article as:
Ghanaee, R., and Akbari Foroud, A. (2026) Economic Assessment and Optimal Sizing of Energy and Storage Systems of a Grid-Connected Turbo-Expander Based Microgrid with Simultaneous Recovery of Cooling and Electrical Energy at Natural Gas Pressure Reduction Stations. *Journal of Modeling & Simulation in Electrical & Electronics Engineering (MSEEE). Semnan University Press* . *6 (3), 1-9.*
DOI: https://doi.org/10.22075/mseee.2026.40212.1244

simultaneously recovering the mechanical exergy of high-pressure NG to drive an electric generator coupled to the TE [2], [3].

As the NG pressure decreases, the Joule–Thomson effect inevitably leads to a reduction in NG temperature. The temperature drop achieved by a TE is significantly greater than that obtained using a conventional pressure regulator [4], which represents an additional advantage of this equipment. The cold NG exhaust from the TE can be routed through a heat exchanger to recover cooling energy [5]. Consequently, the simultaneous recovery of electrical and cooling energy using a TE becomes feasible.

Based on these characteristics, the TE can be considered a suitable alternative for application in microgrids. In recent years, microgrids have attracted increasing attention due to the growing integration of distributed energy resources (DERs) and the need to enhance power quality and energy security, particularly for critical loads. A microgrid is generally defined as a low-voltage distribution network comprising aggregated loads, DERs, and energy storage systems (ESSs), capable of operating in both grid-connected and islanded modes. Various types of energy resources, including dispatchable and non-dispatchable units, can be incorporated into microgrids. Commonly adopted resources include diesel generators, ICEs, microturbines, fuel cells, wind turbines, biomass-based systems, PV systems, and combined heat and power (CHP) units [6]– [11].

A TE is a centrifugal or axial-flow turbine in which high-pressure NG expands and releases energy. In practice, TEs have been employed in air separation processes since the second half of the twentieth century. Owing to their high efficiency and reliability, the application of this technology has gradually become widespread worldwide [12], [13]. The utilization of cooling energy recovered from TEs has a longer history compared to electrical energy recovery. Initially, TEs were predominantly used for cooling energy extraction, while their application for electrical energy generation was developed in later stages.

Existing studies on TEs can be broadly classified into several major categories, including modeling approaches, technical and economic analyses, and methods for supplying energy for NG preheating [14]. From a network perspective, most of these studies model the TE as a distributed generation (DG) unit and focus solely on electrical energy recovery [12]. Given the well-known advantages of microgrids, integrating a TE within a microgrid framework enables the exploitation of its full potential. Moreover, such integration can enhance economic attractiveness and encourage investment in this technology. However, to the best of the authors' knowledge, the application of TEs in microgrids with the simultaneous recovery of both cooling and electrical energy has not yet been investigated.

The selection of the type and capacity of energy generation and storage systems in a TE-based microgrid, similar to conventional microgrids, is of critical importance when considering technical, economic, and environmental factors. However, owing to the unique characteristics of TE-based microgrids discussed in the previous sections, the optimal sizing of energy and storage systems becomes more complex and requires further investigation. Numerous studies have addressed the optimal sizing of microgrid energy resources to satisfy load demands while minimizing annual cost.

In [6], the optimal design of a stand-alone microgrid was presented using a novel multi-objective optimization framework based on the PSO algorithm, to minimize reliability and cost indices. An enhanced multi-objective optimization method for the optimal sizing of all microgrid components was proposed in [8]. In [9], the design of a distributed energy system under uncertainty in a neighborhood environment was investigated. Li et al. [10] developed an optimization model for a combined cooling, heating, and power (CCHP) system, incorporating energetic analysis, economic operation, and environmental impacts.

More recently, a novel grid-connected microgrid configuration based on a TE was proposed in [14], in which optimal capacity sizing and economic analysis were also conducted. However, to prevent hydrate formation, NG is preheated prior to entering the TE in [14]. Consequently, only the recovered electrical energy from the TE can be utilized, while the recovery of cooling energy from the cold NG exhaust is not feasible in that configuration. Compared with reference [14], we have developed a new configuration of a microgrid based on TE. In this new configuration, due to the unique characteristics of the expansion turbine, electrical energy and cooling energy can be simultaneously recovered by the expansion turbine and used in the microgrid.

Previous studies mainly focused on conventional microgrids, CCHP systems, or optimal energy management strategies. Although ref. [14] introduced a TE-based microgrid, the recovered cooling energy was not utilized because natural gas preheating was required before expansion. In contrast, the proposed study introduces a novel TE-based microgrid capable of simultaneously recovering electrical and cooling energy from natural gas pressure reduction stations. Furthermore, a comprehensive mathematical model of the TE, a dedicated optimal sizing framework considering the unique operational characteristics of the TE, and a complete techno-economic assessment including NPV, IRR, and payback period analyses are presented. Therefore, the proposed work extends the existing literature by providing a more comprehensive and economically viable TE-based microgrid configuration.

Table I summarizes the main differences between the proposed study and the most relevant literature.

In this study, the optimal sizing of energy generation and storage systems in a TE-based microgrid is conducted to satisfy cooling, heating, and electricity demands. The objective function is defined as the minimization of the annualized initial capital investment and operation and maintenance (O&M) costs. To this end, an optimal sizing framework is developed that explicitly incorporates the TE. For the economic evaluation of the proposed microgrid, several assessment criteria, including net present value (NPV), internal rate of return (IRR), and payback period (PP), are employed. The performance of the proposed TE-based microgrid is subsequently compared with that of a conventional microgrid without a TE.

The main contributions of this work are summarized as follows:

TABLE I
Comparison of the Proposed Study with the Most Relevant Literature.

Features	[6]	[8]	[9]	[10]	[11]	[14]	[16]	[17]	This work
Grid-connected microgrid	✓	✓	✓	✓	✓	✓	✓	✓	✓
TE integration	✗	✗	✗	✗	✗	✓	✗	✗	✓
Simultaneous recovery of electrical and cooling energy	✗	✗	✗	✗	✗	✗	✗	✗	✓
Detailed TE mathematical model	✗	✗	✗	✗	✗	Partial	✗	✗	✓
TE-based optimal sizing formulation	✗	✗	✗	✗	✗	Partial	✗	✗	✓
Multi-objective optimization	✓	✓	✗	✓	✓	✓	✓	✓	✓
CCHP (electricity-heating-cooling) modelling	Partial	Partial	✓	✓	✓	Partial	✗	Partial	✓
Energy storage modelling	✓	✓	✗	✗	✓	✓	✗	✓	✓
Comparative study (with and without TE)	✗	✗	✗	✗	✗	✗	✗	✗	✓
Cash-flow analysis (NPV, IRR, PP)	✗	✗	✗	✗	✗	Partial	✗	✗	✓
Environmental (CO_2 emission) analysis	Partial	Partial	Partial	✓	✓	✓	✗	✗	✓
Export of surplus electricity to utility	✗	✗	✗	✗	Partial	Partial	✗	✓	✓

1) A novel configuration for grid-connected microgrids based on a TE is proposed for application in pressure regulating stations (PRSs), in which the recoverable electrical and cooling energy from the TE is utilized to supply all or part of the energy demand of the PRSs. Additionally, depending on operational conditions, any excess energy can be exported to the utility grid.

2) Owing to the distinctive characteristics of the TE, including the independence of NG flow rate through the TE from the microgrid energy demand, the non-dispatchable nature of the recoverable electrical and cooling energy, and the simultaneous generation of both cooling and electrical energy, an innovative procedure for the optimal sizing of energy generation and storage systems in a TE-based microgrid is proposed. This procedure incorporates an enhanced multi-objective optimization framework for optimal sizing, combined with a comprehensive cash flow analysis. Furthermore, the economic feasibility of the proposed microgrid is evaluated using relevant financial indicators.

3) A detailed model of TE with a mathematical formulation to calculate the recoverable cooling and electrical energy by TE is presented. Also, the objective function and constraints by considering the role of TE are developed.

The remainder of this paper is organized as follows: The next section provides a brief overview of cooling and electrical energy recovery systems in PRSs. The structure of the proposed TE-based microgrid is demonstrated in Section III. Section IV describes the problem statement, system modeling, and innovative multi-objective optimization algorithm. Section V provides simulation results with and without TE in the proposed microgrids. The discussion of obtained results presents in section VI. Section VII is devoted to a conclusion.

II. The Cooling and Electrical Energy Recovery System in PRSs

In conventional pressure regulating stations (PRSs), the mechanical exergy of high-pressure natural gas (NG) is entirely wasted as heat. A portion of this work potential can, however, be recovered using a TE. When the NG pressure is reduced by either a pressure regulator or a TE, its temperature decreases. The temperature drop achieved by a TE is significantly greater than that of a conventional pressure regulator.

Water content in the NG stream is a critical factor in transmission systems. If the temperature drop exceeds allowable limits, water molecules may react with hydrocarbons to form hydrates [5]. Hydrate formation poses serious operational risks, including pipe and pressure regulator blockages and turbine blade corrosion [2]–[5]. The configuration of a traditional PRS is shown in Fig. 1(a) [5]. High-pressure NG at ambient temperature enters the PRS, after which it is heated by an AB in a process referred to as NG preheating. Finally, the NG exits the PRS and enters the local distribution network.

The modified configuration with the installation of a TE is illustrated in Fig. 1(b) [5]. In this system, the preheating process is replaced by a water removal process. High-pressure NG at ambient temperature enters the PRS, and its water content is reduced to an appropriate level. Consequently, the temperature drop during pressure reduction by the TE does not lead to hydrate formation. The dry NG pressure is reduced below ambient temperature, and before leaving the PRS, its temperature is adjusted to a suitable level for distribution network use. The cold NG exhaust from the TE passes through a heat exchanger to recover cooling energy. This cooling energy can be transferred to a secondary fluid or directly utilized in applications such as space cooling, ethylene plants, refineries, and air separation processes. In this configuration, simultaneous generation of electricity and cooling energy using the TE is possible. To maintain system reliability, the TE is installed in parallel with the existing pressure regulator.

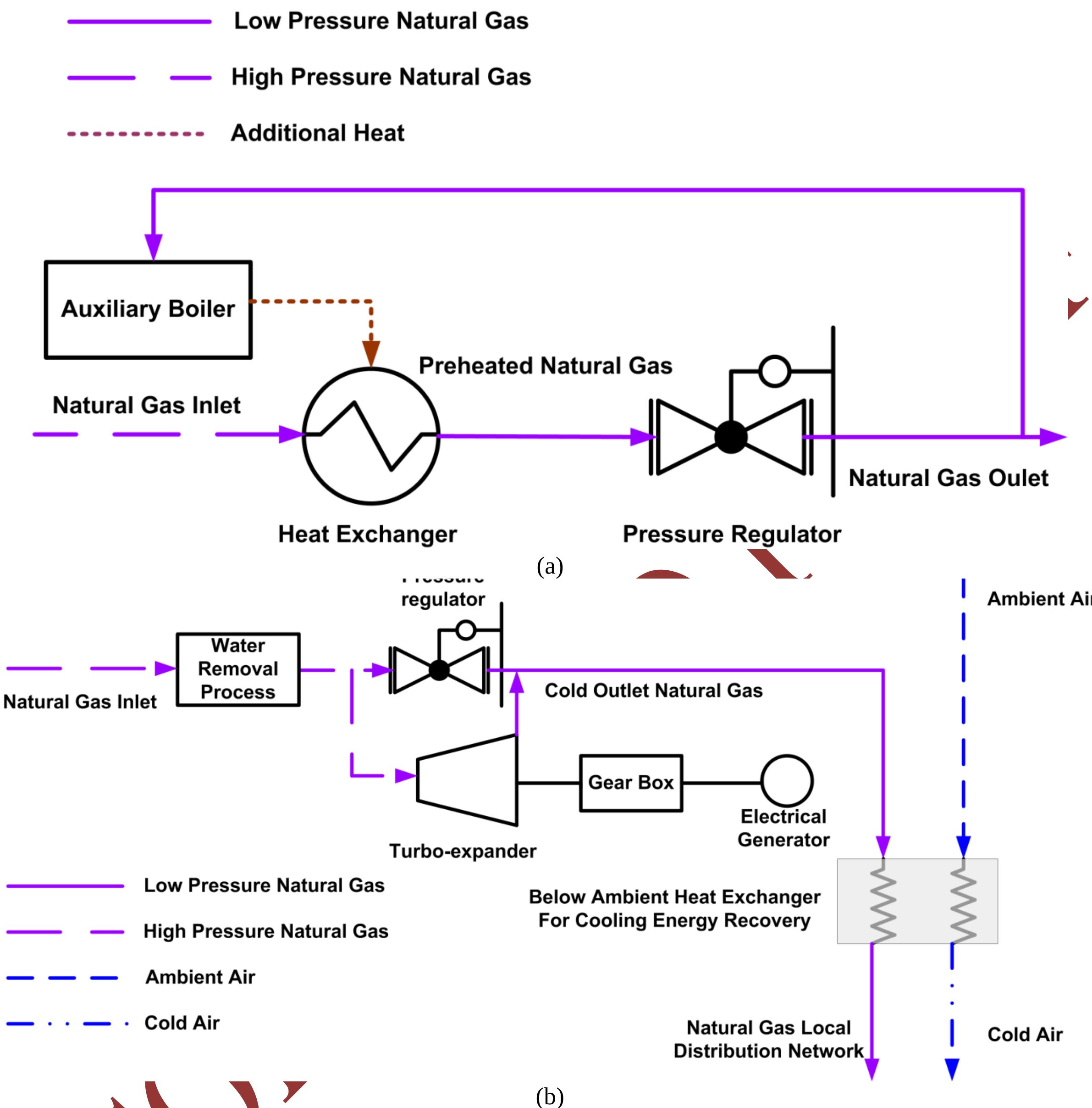

Fig. 1. (a): Conventional PRS (b): The revised system of PRS

III. THE STRUCTURE OF THE PROPOSED TE-BASED MICROGRID

The configuration of the proposed grid-connected TE-based microgrid is illustrated in Fig. 2. This microgrid can be deployed within a pressure regulating station (PRS), where the recoverable electrical and cooling energy from the TE meets a portion of the microgrid's energy demand. The aim is to satisfy the cooling, heating, and electricity energy demand of multi-office buildings, placed in the mentioned industrial plant. The heating, cooling, and electrical load profiles of multi-office buildings of an industrial plant over a period of 20 years are assumed to be constant. In case of energy consumption growth in the coming years, excess energy will be provided by the grid. In addition, it is possible to add the load variation to system modeling. The primary energy source is an internal combustion engine (ICE) operating as a CHP system to generate electricity, heating, and cooling from natural gas. The heat demand is divided into two main categories: hot water and space heating, with the heat storage tank (HST) serving exclusively for hot water storage. An AB is available to supply additional heat if the combined output from the CHP system and HST is insufficient.

For cooling, an AC and an EC are used as backup when the recoverable cooling energy from the TE cannot fully meet the demand. The AC utilizes recoverable heat from the CHP system or additional heat produced by the AB. The microgrid is connected to the utility grid, allowing it to purchase electricity when local generation is insufficient or export surplus electricity. PV panels are considered non-dispatchable energy resources in the system. A BB is incorporated to supply critical loads during any interruption in microgrid or utility operation, and, depending on the state of charge (SOC), it can also supply normal loads.

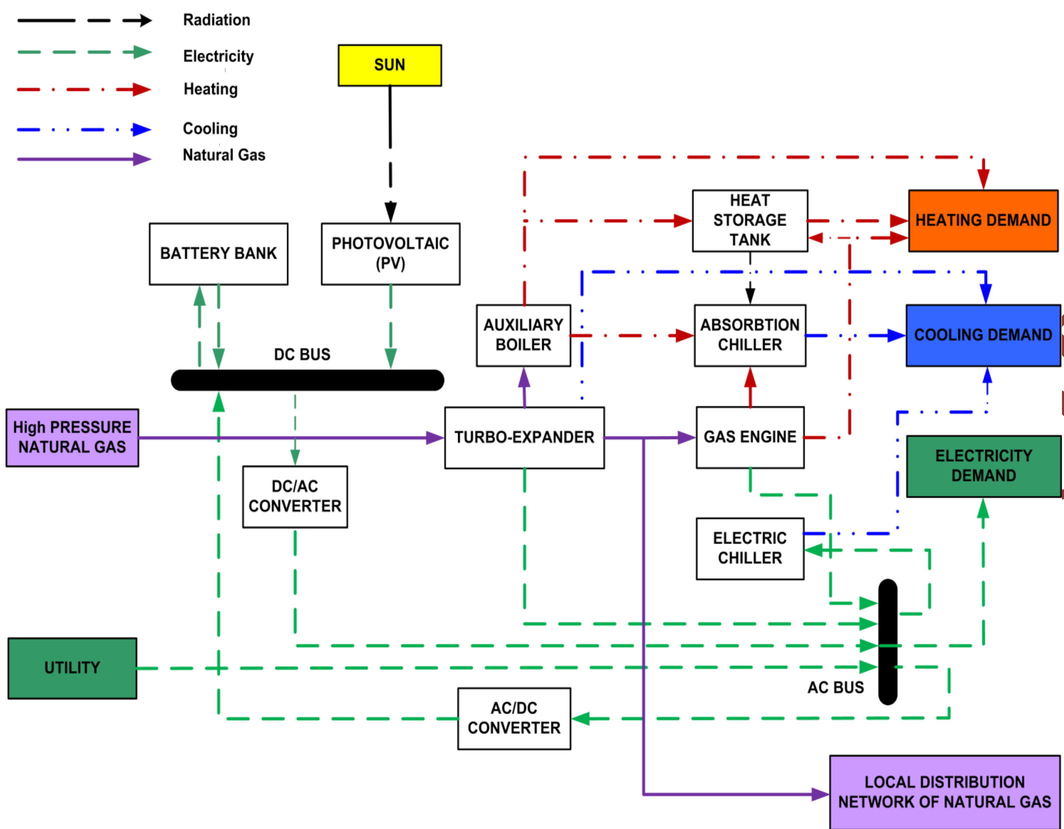

Fig.2. Structure of the proposed grid -connected TE-based microgrid

IV. Mathematical Formulation

In this section, an innovative model is presented for the optimal sizing of energy resources of the proposed TE-based microgrid.

A. Modeling of energy systems

1. TE

The simplified topology of PRS for cooling and electrical energy recovery by TE is shown in Fig. 1b. The model outputs include the rate of recoverable cooling and electrical energy, as well as the outlet NG temperature of TE.

The outlet NG temperature of TE can be computed as follows [15]:

$$T_2 = T_1\left(\frac{P_2}{P_1}\right)^{\frac{k-1}{k}} \quad (1)$$

In (1), P_1, P_2 , T_1 and T_2 are the inlet pressure, outlet pressure, inlet temperature, and outlet temperature of NG passing through TE, respectively, and k is the isentropic constant.

The electrical power recovered by TE is calculated as follows [4]:

$$\dot{P}_{TE,e} = \dot{m}(h_1 - h_2).\eta_{te} \quad (2)$$

where h_1 and h_2 (Fig. 1b) are the enthalpies of points 1 and 2, respectively, $\dot{m}$ is the mass flow rate of NG and η_{te} is the isentropic efficiency of TE.

The cooling power recovered can be computed using the NG enthalpy difference between the PRS exit point (h_{ep}) and the outlet of TE (h_2) as follows [5]:

$$\dot{P}_{TE,c} = \dot{m}(h_{ep} - h_2).\eta_{he} \quad (3)$$

where η_{he} is the heat exchanger efficiency.

2. CHP system

In the current paper, an ICE as a CHP system is considered. The electrical efficiency ($\eta_{e,ICE}$) and heat recovered from ICE ($P_{h,ICE}$) depends on its nominal electrical power ($P_{e,ICE}$), which is calculated as follows [16]:

$$\eta_{e,ICE} = 0.232.\left(P_{e,ICE}\right)^{0.084} \quad (4)$$

$$P_{h,ICE} = 2.5.\left(P_{e,ICE}\right)^{0.91} \quad (5)$$

3. Photovoltaic

The output power of a PV is described using [17]:

$$P_{PV}(t) = N_{PV}.\eta_{PV}.A_{PV}.G_A(t) \quad (6)$$

where N_{PV} is the number of panels, η_{PV} is the efficiency of PV panels, A_{PV} is the area of a single panel (m^2) and G_A is the global solar radiation (w/m^2).

4. Battery bank

In this paper, a lead-acid battery is considered the electrical storage system. Due to the limitations of the charging and discharging rate of BB, the following constraints should be satisfied in each time interval [11], [18]:

$$SOC(t) = SOC(t-\Delta t) + \Delta t\left(\eta_c P_{bc}(t) - \frac{P_{bd}(t)}{\eta_d}\right) \quad (7)$$

$$SOC_{min}(t) \le SOC(t) \le SOC_{max}(t) \quad (8)$$

where $SOC(t)$, $SOC(t-\Delta t)$, $SOC_{min}(t)$, $SOC_{max}(t)$, Δt, η_c, η_d, P_{bc}, P_{bd} are SOC at time t and $t-\Delta t$, min/max SOC for BB, simulation time interval, BB charging/discharging efficiency, and BB charging/ discharging power, respectively.

5. Heat storage tank

HST for space heating is considered to minimize the use of AB, which is a water-based system.

6. Auxiliary boiler

In the proposed microgrid, an AB might be brought into service if the balance of heating demand is not completely satisfied by the CHP system and HST. It is assumed that AB has an efficiency of 90%.

7. Absorption chiller

The single-stage lithium bromide ACs offer cost-efficient chilled-water cooling using waste heat [19]. In the proposed microgrid, the cooling load that is not served by cooling energy recoverable by TE is served by AC. The coefficient of performance (COP) of AC is assumed to be 0.7. The electricity consumption of AC is assumed to be 10% of the equivalent EC [20].

8. Electric chiller

In addition to TE and AC, an EC is considered to meet the cooling load during peak load hours. The value of three is assumed for the COP of an EC [21].

B. Input profiles

The hourly variations of the NG flow rate in the PRS, as well as the cooling, heating, and electricity load profiles for the case study over one year, are presented in Figs. 3(a)–3(d), respectively. All days of each month are considered representative, and the load profiles are assumed to remain constant over a 20-year period. Any shortfall in electrical energy will be supplied by the utility in the event of future load growth. A standard working day from 7:30 a.m. to 5:00 p.m. is assumed. The heat demand includes hot water throughout the year and space heating during the winter months. The cooling demand covers both space cooling and refrigeration facilities. The electricity demand accounts for electrical appliances and lighting over the entire year.

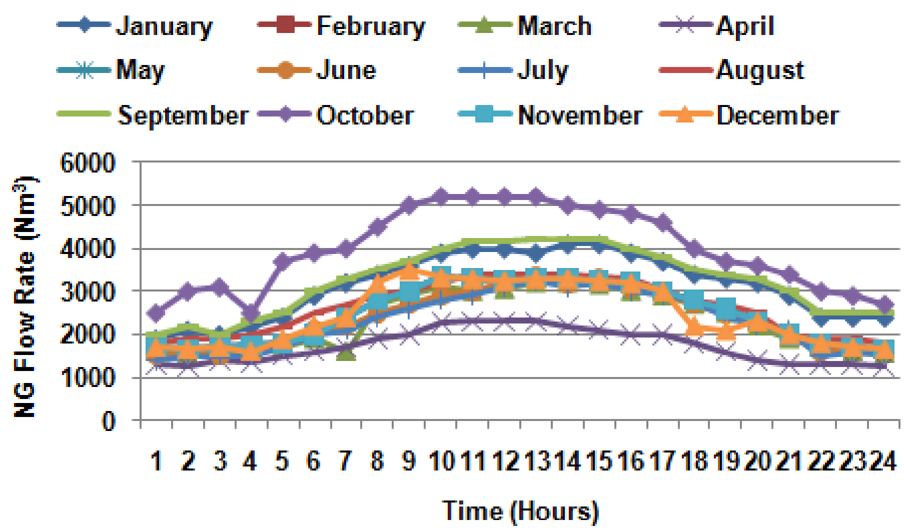

(a)

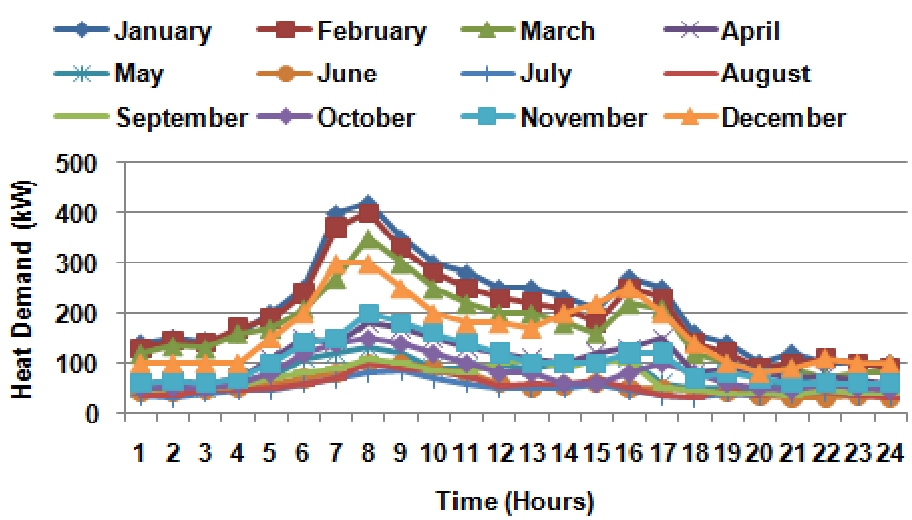

(b)

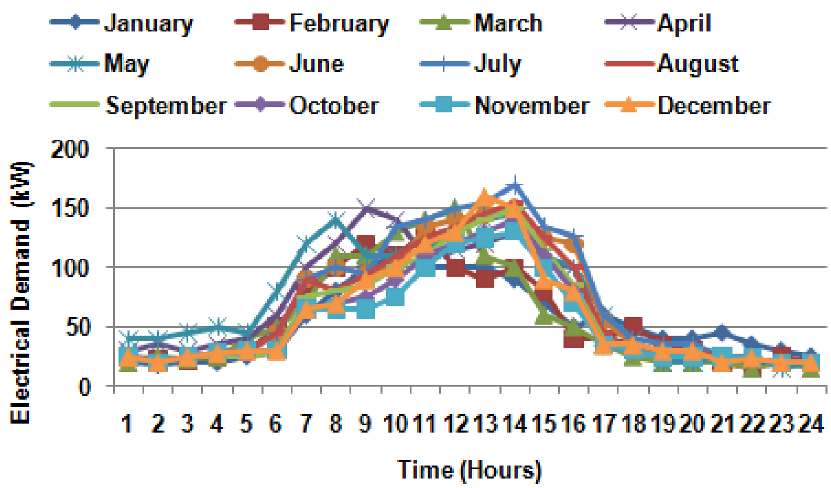

(c)

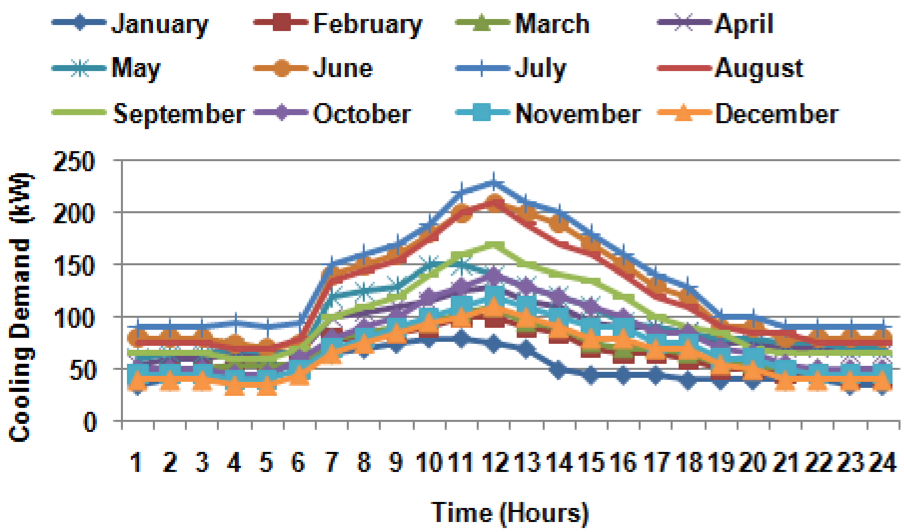

Fig. 3. Input profiles (a): NG flow rate variation, (b): Heat load profile, (c): Electrical load profile, (d): Cooling load profile

C. The Flowchart of Optimization Algorithm

The flowchart of the proposed multi-objective optimization algorithm for the optimal sizing of energy generation and storage systems in a TE-based microgrid is presented in Fig. 4. This framework enables decision-makers to select the most appropriate configuration by considering trade-offs among multiple objectives. In this study, the multi-objective optimization problem focuses on economic aspects, including the minimization of initial capital and operation and maintenance (O&M) costs, as well as environmental considerations, such as emissions, subject to operational constraints.

The proposed algorithm consists of three main stages: TE sizing, optimal sizing of energy and storage systems using the PSO algorithm, and economic analysis. The initialization stage involves calculating the recoverable electrical and cooling energy from the TE based on hourly input data. Since the primary function of the TE is pressure reduction, its nominal size is determined according to the computed electric power. Specifically, the TE size is set based on the NG flow rate passing through it, which is proportional to the required NG in the distribution network rather than the microgrid energy demand.

These results are then applied to the optimal sizing problem to determine the type and size of other energy and storage systems, excluding the TE. The objective function of this optimization is to minimize both the annualized initial capital and O&M costs, which is solved using the PSO algorithm. A full-year operation simulation is conducted to evaluate the performance of the proposed microgrid under expected demand profiles. Finally, an economic analysis is performed at the optimal solution. If the economic indicators are unsatisfactory, fine-tuning the weighting and penalty factors in the objective function can yield improved results (Fig. 4). The design variables considered include the PV surface area and the nominal sizes of the ICE, AB, AC, EC, BB, and HST. The following sections provide detailed descriptions of the proposed optimal sizing algorithm. The Important parameters of the PSO algorithm have been determined based on trial and error.

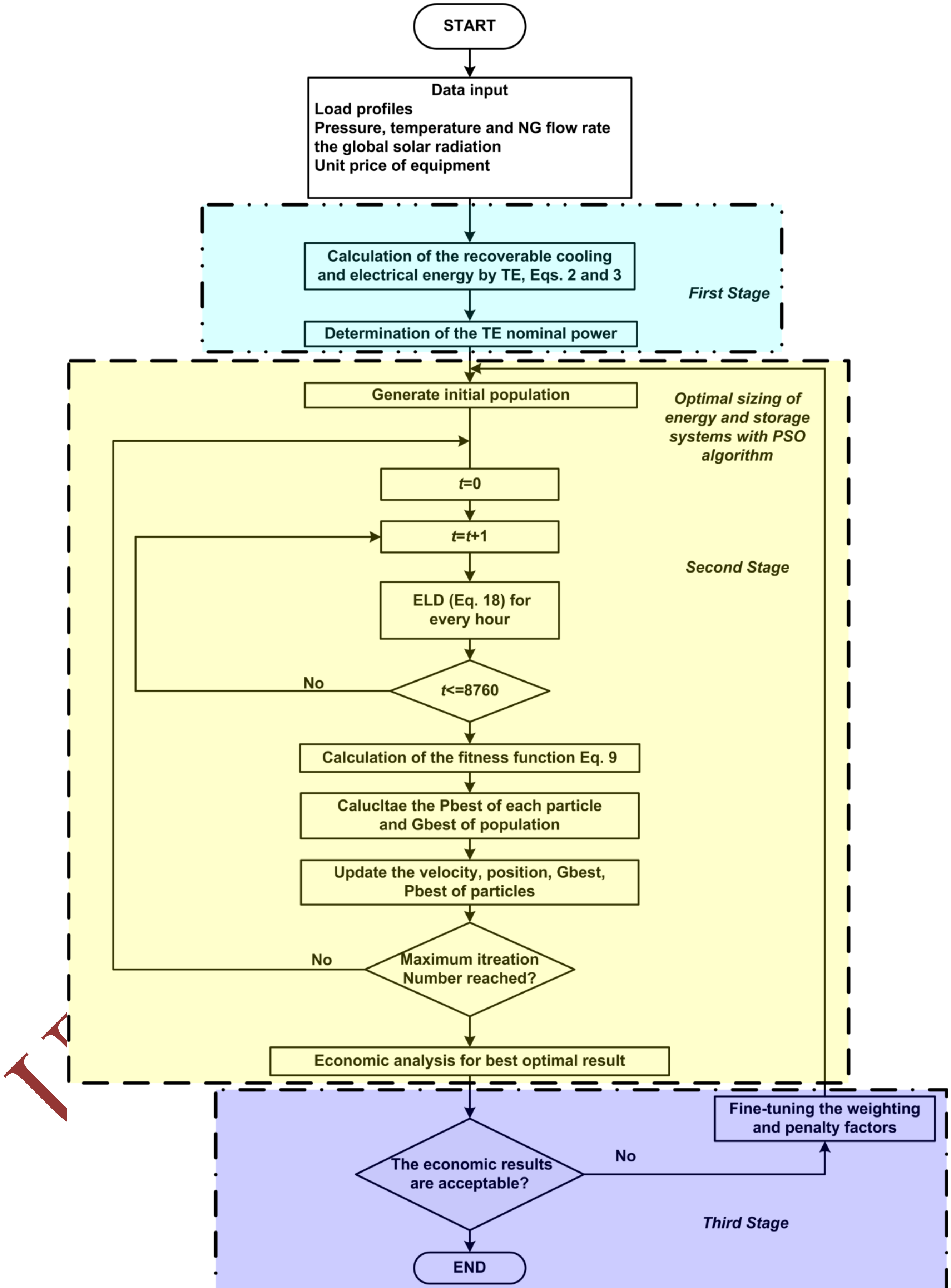

Fig.4. The flowchart of the multi-objective algorithm for optimal sizing of energy and storage systems in a TE-based microgrid.

1. Objective function

In the current paper, the objective function of the optimal sizing problem is to minimize the present value of all costs, which should be developed according to the role of TE as follows:

$$C = w_1 . C_{inv} + w_2 . \sum_{m=1}^{365} \sum_{t=1}^{24} C_{OM} + \mu_1 . E_{e,u} + \mu_2 . E_{h,sh} + \mu_3 . E_{h,su} + \mu_4 . E_{c,sh} \quad (9)$$

The first term in (9) is the total initial capital cost (C_{inv}) and it includes the installation cost, considering technologies as follows:

$$C_{inv} = \sum_{i=1}^{n} CRF_i . C_i \quad (10)$$

where CRF_i and C_i are the capital recovery factor and initial capital cost for component *i*, respectively.

The capital recovery factors are calculated as follows:

$$CRF(i_r, R) = \frac{i_r \times (1+i_r)^R}{(1+i_r)^R - 1} \quad (11)$$

where R is the lifetime of each technology and i_r is the real interest rate, which is a function of the nominal interest rate (i_{rn}) and annual inflation rate (i_f) as follows [22]:

$$i_r = \frac{i_{rn} - i_f}{1 + i_f} \quad (12)$$

C_{OM} in (9) is O&M costs, which includes fuel gas cost (C_{FG}), emission cost (C_{EM}), the maintenance cost (C_M) and the cost of the purchased electricity from the utility ($C_{e,u}$) as follows:

$$C_{OM} = C_{FG} + C_{EM} + C_M + C_{e,u} \quad (13)$$

Fuel gas cost consists of fuel gas for the ICE ($C_{FG,ICE}$) and AB ($C_{FG,AB}$) as follows:

$$C_{FG} = C_{FG,ICE} + C_{FG,AB} = \sum_{t=1}^{8760} \Big(\big(P_{e,ICE}(t) / \eta_{e,ICE} \big) + \big(P_{AB}(t) / \eta_{AB} \big) \Big) \times \alpha_{NG} \quad (14)$$

In which, $P_{AB}(t)$, η_{AB} and α_{NG} are the output power of AB, the heat efficiency of AB, and the price of NG ($/kWh), respectively.

In this study, we only consider CO_2 emissions from purchased electricity from the utility ($C_{EM,u}$), ICE ($C_{EM,ICE}$), and AB ($C_{EM,AB}$). The emission cost can be computed as follows:

$$C_{EM} = C_{EM,ICE} + C_{EM,AB} + C_{EM,u} = \sum_{t=1}^{8760} \Big(\Big(\big(P_{e,ICE}(t) / \eta_{e,ICE} \big) + \big(P_{AB}(t) / \eta_{AB} \big) \Big) . \beta_{EM,NG} + \big(P_{e,u}(t) . \beta_{EM,u} \big) \Big) . \alpha_{EM,NG} \quad (15)$$

which, $\beta_{EM,NG}$, $\beta_{EM,u}$, $P_{e,u}(t)$ and $\alpha_{EM,NG}$ are the NG emission factor, utility electricity emission factor, electrical power taken from the utility, and the cost of CO_2 emission ($/Ton), respectively.

The maintenance cost is as follows:

$$C_M = \sum_{i=1}^{n} C_{i,M} \quad (16)$$

where $C_{i,M}$ is the maintenance cost of component *i*.

Finally, the total cost for power purchased from the utility for a year can be calculated as follows:

$$C_{e,u} = \sum_{t=1}^{8760} P_{e,u}(t) . \alpha_{e,u} \quad (17)$$

where, $\alpha_{e,u}$ is the price of utility electricity.

$E_{h,sh}$, $E_{c,sh}$ and $E_{h,su}$ are annual heat energy shortage, annual cooling energy shortage, and annual heat energy surplus, respectively. In addition, μ_2, μ_3 and μ_4 are penalty factors for shortage heating, surplus heating, and shortage cooling demands ($/kWh), respectively. The last term is related to the penalty cost, which is added to the objective function to meet the electricity demand of the microgrid by microgrid energy resources as far as possible, which μ_1 is the penalty factor and $E_{e,u}$ is the annual electrical energy taken from the utility. Furthermore, w_1, w_2 in (9) are considered weighting factors for initial capital and O&M costs, respectively.

2. Economic Load Dispatch (ELD)

In stage 2 of the proposed multi-objective algorithm, economic load dispatch should be performed for every hour of the year, with the objective function being the minimization of O&M costs as follows:

$$C_{ELD} = C_{OM} \quad (18)$$

3. Constraints

The constraints are developed based on the role of TE. A physical constraint that should be considered is the available surface area for PV installation ($A_{PV,t}$) as follows:

$$A_{PV,MIN} \leq A_{PV,t} \leq A_{PV,MAX} \quad (19)$$

where $A_{PV,MIN}$ and $A_{PV,MAX}$ are the minimum and maximum allowable areas for PV installation, respectively.

The cooling, heating, and electrical energy should be balanced on each hour as follows:

$$E_{D,e} + E_{ED,AC} + E_{D,EC} = E_{PV} + E_{TE,e} + E_{ICE,e} + E_{BB} + E_u \quad (20)$$

$$E_{D,SH} + E_{D,HW} + E_{D,AC} = E_{ICE,h} + E_{AB} + E_{HST} \quad (21)$$

$$E_{D,c} = E_{AC} + E_{TE,c} + E_{EC} \quad (22)$$

where E_{PV}, $E_{TE,e}$ and $E_{ICE,e}$ are the electrical energy produced by PV, TE, and ICE, respectively. E_{BB} is the BB charging/ discharging energy and E_u is the electrical energy from/to the utility. On the left side, $E_{D,e}$, $E_{D,AC}$ and $E_{D,EC}$ are the electricity demands of the microgrid, AC and EC, respectively. In (21), on the left side, is shown the demand for heat energy (for space heating ($E_{D,SH}$), hot water ($E_{D,HW}$) and AC ($E_{D,AC}$)). On the right side, heat recovered from ICE ($E_{ICE,h}$), heat energy production by AB (E_{AB}) and heat energy from/to HST (E_{HST}) are shown. Finally, (22) shows the energy balance for the cooling energy that $E_{D,c}$ is the demand for cooling energy, including space cooling and refrigeration facilities. On the right side, E_{AC} and E_{EC} are cooling energy production from AC and EC, respectively, and $E_{TE,c}$ is recoverable cooling energy by TE.

The cooling, heating, and electrical energy generated by each energy resource must be in the allowable range as follows:

$$PG_{emin,i} \leq PG_{e,i} \leq PG_{emax,i} \quad (23)$$

$$PG_{hmin,i} \leq PG_{h,i} \leq PG_{hmax,i} \quad (24)$$

$$PG_{cmin,i} \leq PG_{c,i} \leq PG_{cmax,i} \quad (25)$$

D. Equations for economic analysis

Several criteria, including NPV, IRR, and PP, are used in discounted cash flow to estimate project performance.

NPV is used to determine the present value of an investment by the sum of the discounted annual cash flows, which can be calculated as follows [11], [22]:

$$NPV = -C_{inv0} + \sum_{T=1}^{20} \frac{R_n}{(1+r)^T} \quad (26)$$

where r is the discount rate, C_{inv0} is the initial capital cost (without considering the capital recovery factor), T is the project lifetime, and R_n is the annual cash flow (annual revenue minus annual cost).

V. Simulation Results

This section presents the results of the optimal sizing of energy generation and storage systems in the proposed microgrid, both with and without a TE. The inlet pressure and temperature of NG entering the PRS are assumed to be 570 psi and 20 °C, respectively, across the range of flow rates. The outlet NG pressure at the TE is set to 250 psi. Table II summarizes the input data used for the simulations.

In both cases, the objective function is to minimize the annualized initial capital and O&M costs, as expressed in (9). The maintenance costs for the TE, ICE, AB, AC, and EC are assumed to be 0.01, 0.009, 0.00324, 0.02, and 0.02 $/kWh, respectively. Energy prices are also assumed to be constant over a 20-year period. Also, future grid reinforcement costs are not included in the modeling. For PV, BB, and HST, maintenance costs are considered as 0.8%, 2%, and 2% of their initial capital costs, respectively. Additionally, it is assumed that 50% of the initial capital cost of the PV system is subsidized by the government.

TABLE II
Constant Data [22], [23]

Item	Units	Value
Capital cost of TE	$/kW	1500
Capital cost of ICE	$/ kW	1000
Capital cost of PV	$/ kW	4500
Capital cost of AB	$/ kW	125
Capital cost of HST	$/ kW	120
Capital cost of BB	$/Ah	1
Capital cost of AC	$/ kW	400
Capital cost of EC	$/ kW	300
Electricity sold on-site and utility	$/ kWh	0.11
Price of utility electricity	$/ kWh	0.12
Heat sold on-site	$/ kWh	0.05
Cooling sold on-site	$/ kWh	0.09
Lifetime of TE, ICE, AB, HTS, AC, and EC	Year	20
Lifetime of PV	Year	25
Lifetime of BB	Year	5
Price of natural gas	$/ kWh	0.02
Utility electricity emission factor	kg $CO2/\ kWh_e$	0.55
NG emission factor	kg $CO2/\ kWh_e$	0.184
Cost of co2 emission	$/Ton	33

As discussed in previous sections, the nominal sizes of all energy and storage systems, except for the TE, are determined using the PSO algorithm. Following the first step in Fig. 4, the nominal size of the TE and the corresponding recoverable electrical and cooling energy are calculated. These values are then used as inputs for the optimization program. The exhaust NG temperature from the PRS is assumed to be 10 °C. Monthly average cooling and electrical energy recovered by the TE are presented in Table III. The annual average recovered cooling and electrical energy are 44.7 kW and 50.6 kW, respectively, with a peak electrical power of 76 kW occurring in October.

Furthermore, based on the hourly NG flow rate variations shown in Fig. 3, the electrical energy production by the TE reaches a maximum of 99 kW between 10:00 a.m. and 12:00 p.m. in October. Considering that TEs can operate between 50% and 140% of their nominal capacity [24], the nominal size of the TE in this case study is selected as 90 kW.

TABLE III.
Cooling and Electricity Energy Recovery by TE.

Month	*Gas flow rate (Nm^3/h)*	*Recovered electrical energy by TE (kW)*	*Recovered cooling energy by TE (kW)*
April	1725	32.9	29.3
May	2480	47.3	42
June	2375	45.3	40.4
July	2300	44	39
August	2600	52.45	44.3
September	3240	62	55
October	3980	76	68
November	2480	47.3	42
December	2480	47.3	42
January	3130	60	53.3
February	2480	47.3	42
March	2360	45	40

Table IV presents the optimal sizes of the energy generation and storage systems for both cases, as determined by the PSO algorithm. In Case 1, the rated power of the ICE is 91 kW, whereas in Case 2 it increases to 149.5 kW, as 72% of the electricity in Case 1 is supplied by the TE. Despite 50% of the initial capital cost of PV being subsidized by the government, the PV surface area is zero in both cases. The rated power of the BB increases from 3 kW in Case 1 to 186 kW in Case 2, with the lower bound set at approximately 3 kW to supply critical loads during power interruptions.

Both cases include the AB and HST, with their nominal sizes in Case 2 increased relative to Case 1. For cooling, Case 1 utilizes the TE and an AC, whereas Case 2 includes an AC and an EC. On hot days, the AC is the most economical option for providing cooling from the recovered waste heat of the ICE. However, relying on a single energy resource may not be sufficient to meet cooling demands. Therefore, in Case 2, the lower limit of the EC is set to 50 kW in the optimization program, representing the minimum required cooling capacity for emergency loads.

TABLE IV
Sizes of the Energy and Storage Systems for both Cases.

Case No.	*1*	*2*
TE (kW)	90	X
ICE (kW)	91	149.5
PV (m2)	0	0
BB (kW)	3	186
AB (kW)	368	392.5
HST (kW)	50	100
AC (kW)	152	180
EC (kW)	X	50

The annual fractions of cooling, heating, and electricity demands supplied by the various energy and storage systems for both cases are summarized in Table V. In Case 1, the TE directly satisfies 71.4% of the electrical demand and 51% of the cooling demand, with the remaining electrical load supplied by the ICE and the utility. The utility's contribution is minimal due to the penalty factor μ_1 included in the objective function. Additionally, the BB does not participate in meeting normal loads in Case 1, whereas it supplies 7% of the electrical energy in Case 2.

The heat demand, including that required for the AC, is met by the recovered waste heat from the ICE, the AB, and the heat storage tank (HST) in both cases. In Case 1, the ICE provides up to 17% of the annual heat demand, while in Case 2, this fraction increases to 28%. This increase is primarily because Case 2 does not include a TE, requiring a larger ICE capacity to meet the electrical demand. Moreover, in the absence of the TE, additional heat is required for the AC to produce cooling energy. Consequently, the AC's contribution to cooling demand rises from 49% in Case 1 to 99% in Case 2, whereas the EC plays a marginal role, supplying only 1% of the cooling load.

Fig. 5 illustrates the monthly energy production of the systems in Case 1. As shown in Fig. 5(a), the TE operates throughout the year, with the recovered electrical energy peaking in October. Electricity is exported to the utility in all months, while during peak periods, including March, April, and July, electricity is imported from the utility. The ICE operates continuously, and its recovered waste heat is used to supply heating loads and the AC. Fig. 5(b) shows that the AB, as a backup heat source, operates year-round, reaching its maximum output in January, the coldest month. Fig. 5(c) indicates that the cooling energy recovered by the TE is also highest in October.

The monthly energy production for Case 2 is presented in Fig. 6. In this case, the absence of a TE requires a greater share of electrical demand to be met by the ICE, with the remaining demand supplied by the BB and the utility. No electricity is exported to the utility; during peak hours, it is imported as needed. In both cases, the HST plays a moderate role in meeting the heat demand. Fig. 6(c) shows that the AC provides the majority of the cooling energy, while the EC contributes significantly during the warmer months.

Figs. 7 and 8 present the energy demand and supply profiles of the proposed microgrids for a typical day in July. In Case 1, the TE operates continuously throughout the day, with its electrical output peaking around midday. The ICE operates from 6:00 a.m. to 3:00 p.m., directly supplying both heating and electricity demands. The power output of the BB remains constant throughout the day and does not participate in meeting normal loads. Power is exchanged with the utility depending on the demand during peak and off-peak periods. The AB operates at all hours to provide the required heat for space heating, hot water, and the AC.

TABLE V
Annual Fractions of Cooling, Heating, and Electricity Demands Satisfied by Various Energy and Storage Systems (a): Case 1, (b): Case 2.

Energy system	*Annual electrical energy*	*Annual heat energy*	*Annual cooling energy*
TE	71.4%	X	51%
ICE	28.3%	17%	X
PV	X	X	X
Grid	0.3%	X	X
Battery bank	0	X	X
AB	X	72%	X
HTS	X	11%	X
AC	X	X	49%
EC	X	X	X

(a)

Energy system	*Annual electrical energy*	*Annual heat energy*	*Annual cooling energy*
TE	x	X	X
ICE	92%	28%	X
PV	0	X	X
Grid	1%	X	X
Battery bank	7%	X	X
AB	X	52%	X
HTS	X	20%	X
AC	X	X	99%
EC	X	X	1%

(b)

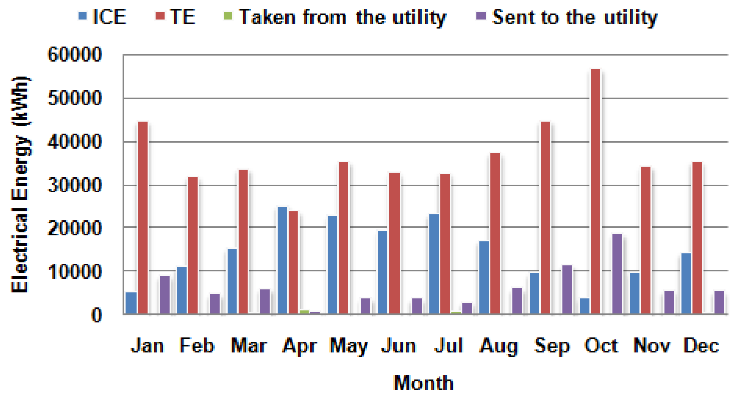

(a)

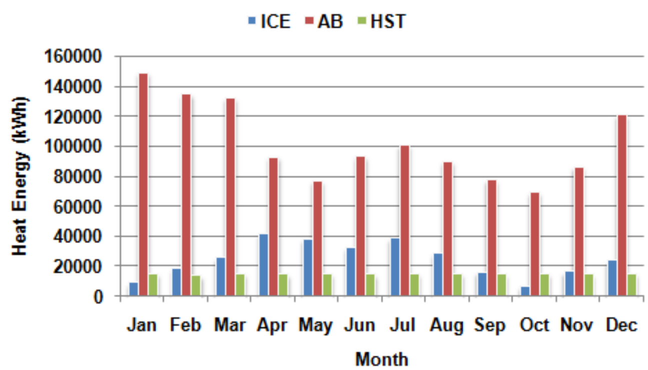

(b)

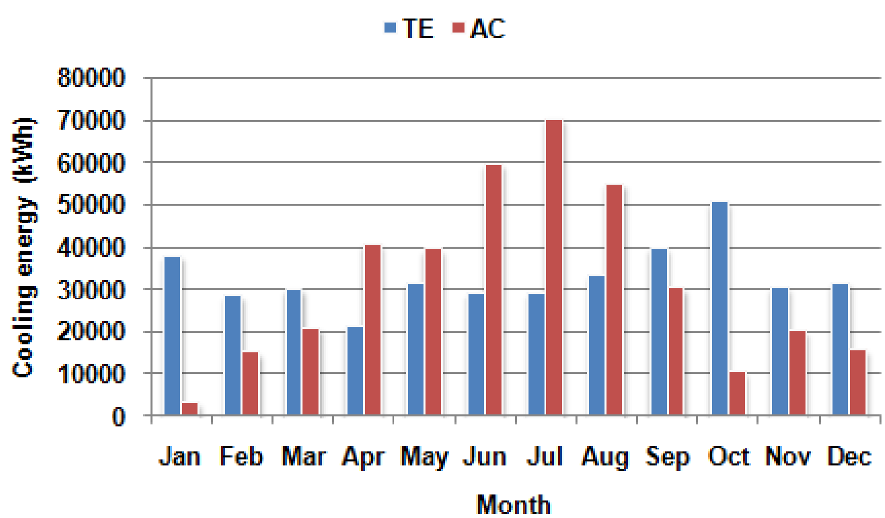

(c)

Fig. 5. Monthly productions of energy and storage systems for case 1 (a): electrical energy, (b): heat energy, (c): cooling energy.

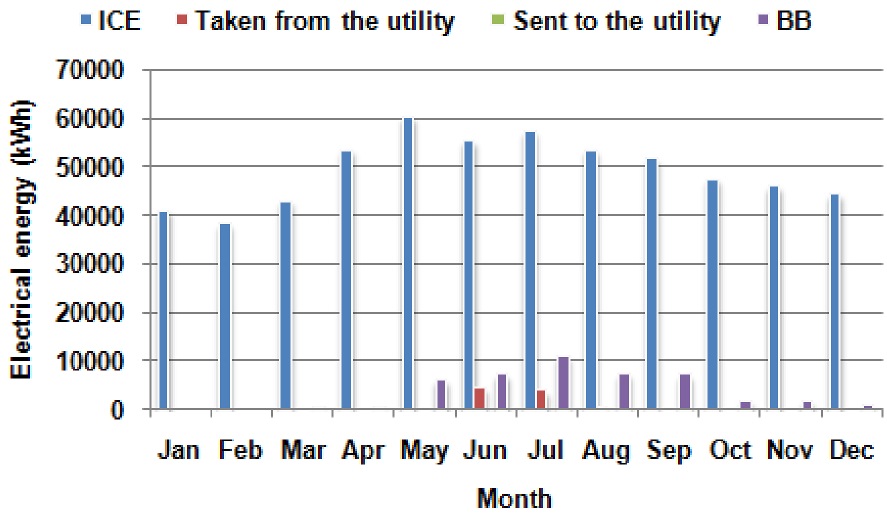

(a)

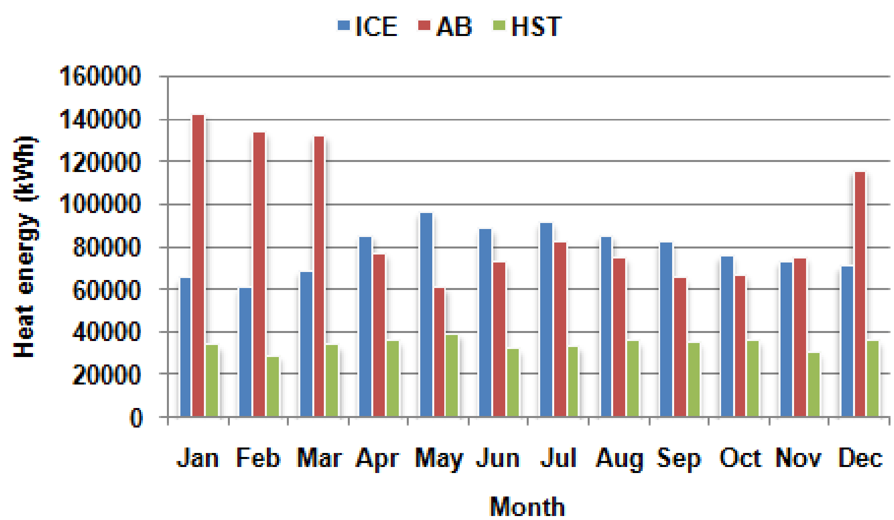

(b)

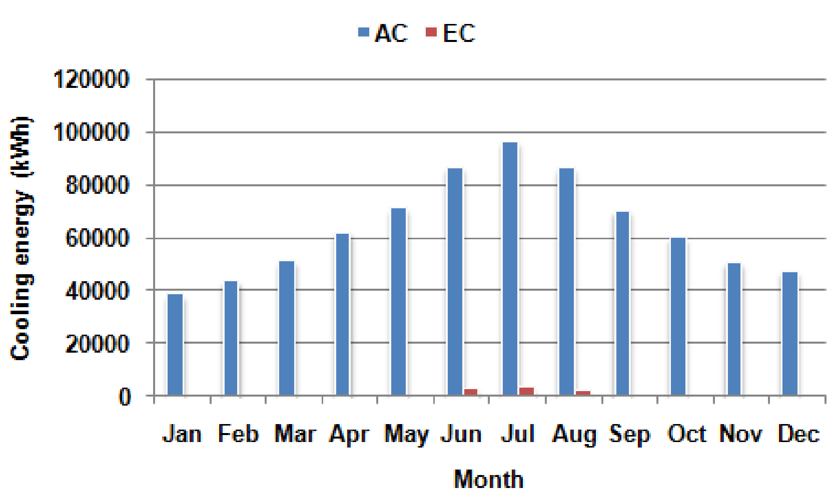

(c)

Fig. 6. Monthly productions of energy and storage systems for case 2 (a): electrical energy, (b): heat energy, (c): cooling energy.

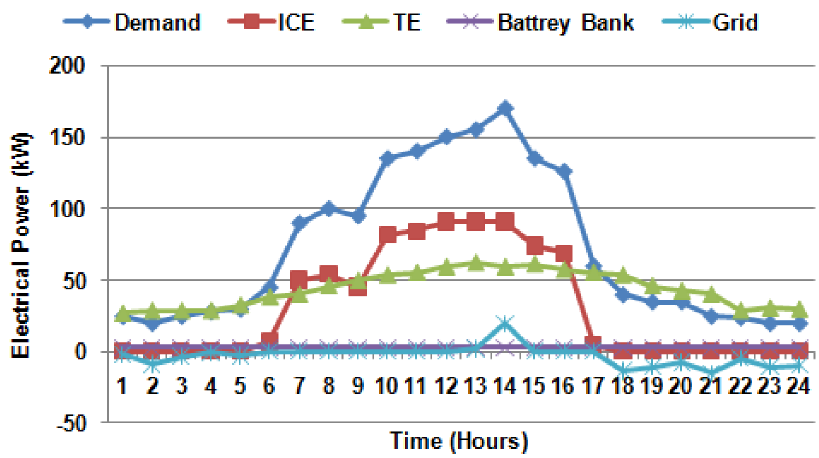

(a)

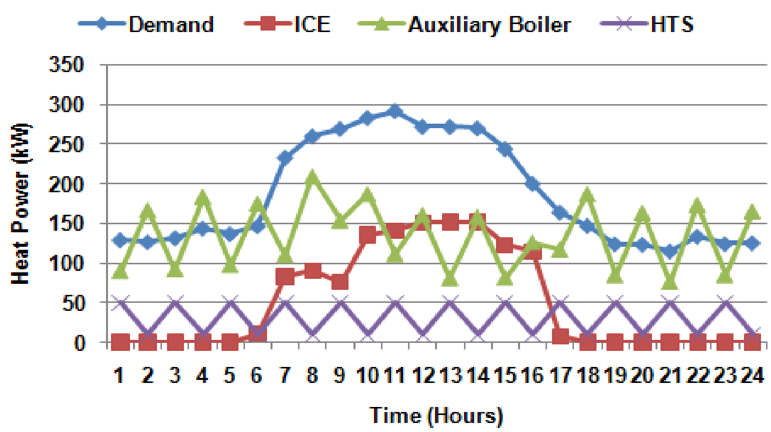

(b)

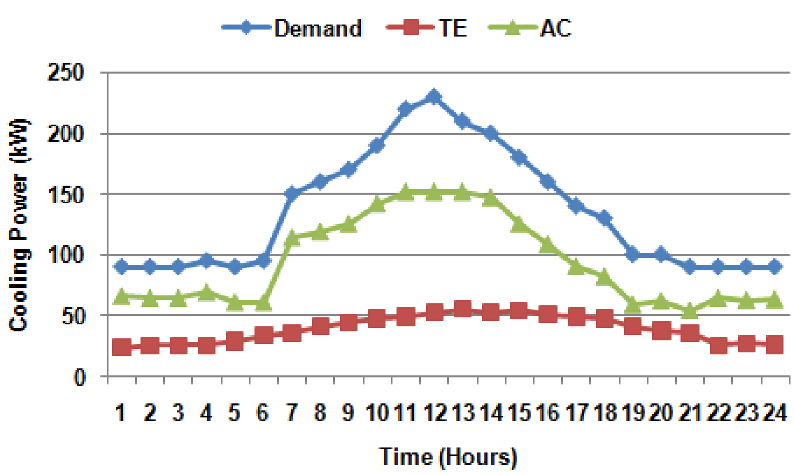

(c)

Fig. 7. Hourly energy production of energy and storage systems for a typical day in June in case 1(a): electrical energy, (b): heat energy, (c): cooling energy.

In Case 2, the ICE operates continuously throughout the day, with its output power peaking between 11:00 a.m. and 3:00 p.m. The BB discharges during the peak period from 11:00 a.m. to 4:00 p.m. and charges during off-peak hours. Electricity is imported from the utility between 11:00 a.m. and 4:00 p.m. based on load demand, while no electricity is exported to the utility at any time. The AB operates intermittently according to the heat demand profile. Due to the absence of a TE and the non-economical use of the EC, the majority of the required cooling energy is supplied by the AC. The EC is only activated during peak hours, from 10:00 a.m. to 3:00 p.m., in accordance with the cooling load profile.

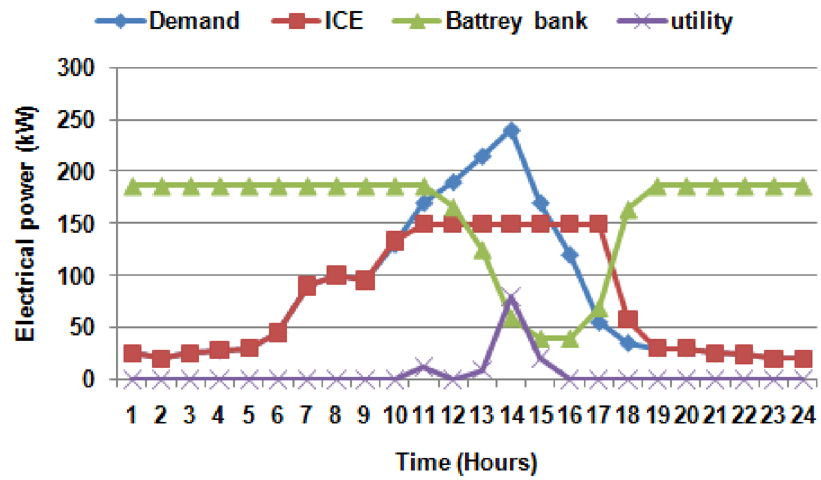

(a)

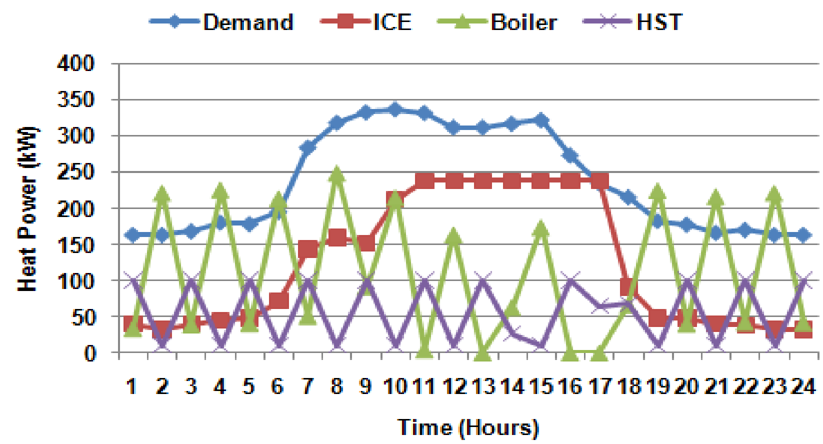

(b)

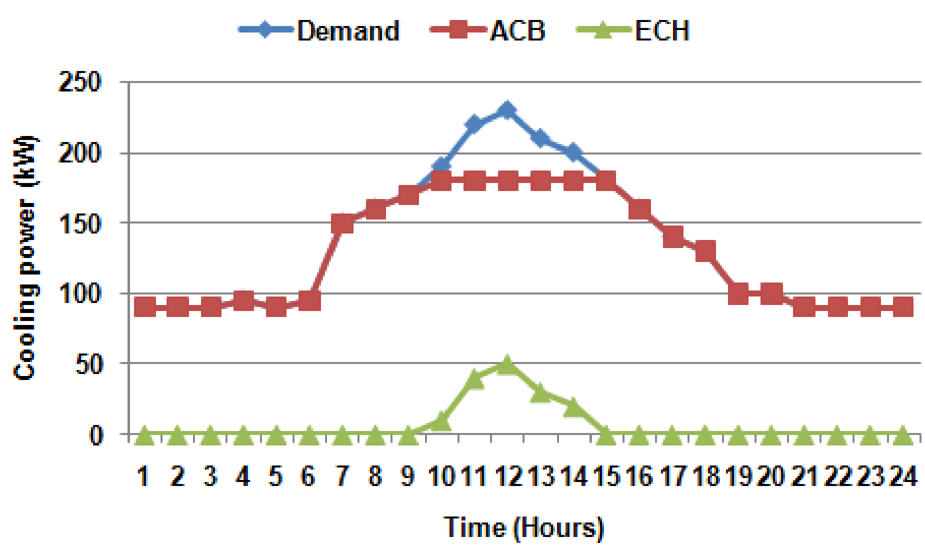

(c)

Fig. 8. Hourly energy production of energy and storage systems for a typical day in June in case 2(a): electrical energy, (b): heat energy, (c): cooling energy.

A. Economical assessment

The economic assessment of the proposed microgrids at their optimal configurations (Table IV) is presented in Fig. 9. Energy sale and purchase tariffs are assumed to remain constant throughout the project lifetime. The initial capital cost in Case 1 is approximately 8% higher than in Case 2, primarily due to the high capital cost of the TE. As shown in Section V, in Case 1, the TE supplies approximately 71% of the electrical demand and 51% of the cooling demand. Since the energy recovered by the TE does not require primary energy input, Case 1 achieves annual reductions of up to 35.2% in emissions and 35.6% in fuel costs compared with Case 2 (without TE).

Furthermore, the maintenance cost in Case 2 is about 28.2% higher than in Case 1, as the TE simultaneously recovers both cooling and electrical energy, resulting in a 34% reduction in O&M costs for Case 1. The annual revenue in Case 1 is slightly higher due to increased electricity sales to the utility, leading to a total annual profit that is 48.6% higher than in Case 2. Cash flow analyses, including NPV, IRR, and PP, were conducted for both cases with a discount rate of 7%. Despite similar initial capital costs, the NPV and IRR in Case 1 are 72% and 38% higher, respectively, compared to Case 2. The payback periods are 2.8 and 4 years for Cases 1 and 2, respectively. The reduced O&M costs in Case 1 due to the TE contribute to the increased annual profit, demonstrating that the TE-based microgrid is economically more advantageous than the conventional microgrid.

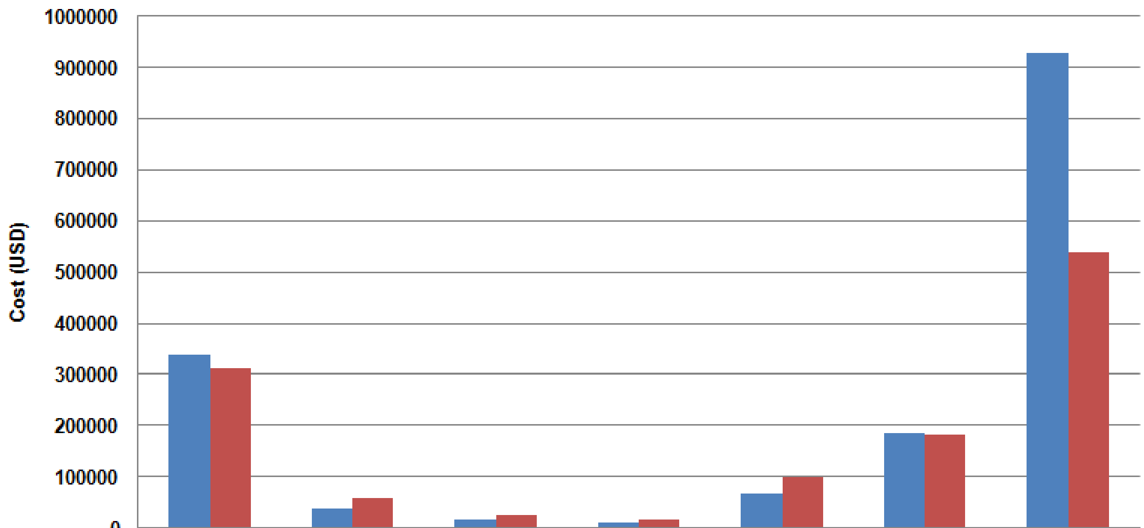

	Total installation cost	Fuel gas cost	Maintenance cost	Emission cost	Total OM cost	Total revenues	NPV
Case 1	339050	37415	17669	11043	66329	185967	928354
Case 2	313062	57750	24782	17152	100706	181183	539496

Fig. 9. Economic analysis based on the PSO algorithm at optimal results.

VI. Discussion

The main objective of this study was to investigate the integration of TEs in microgrids. The key findings regarding TE-based microgrids are summarized as follows:

1. In PRSs, traditional pressure regulators can be replaced with TEs. Therefore, unlike conventional microgrids, TE-based microgrids are specifically suitable for installation in PRSs or other industrial natural gas supply systems.
2. The proposed mathematical model for the optimal sizing of energy generation and storage systems, presented in the previous sections, enables the evaluation of both economic and environmental benefits of TE-based microgrids compared to traditional microgrids without TEs.
3. According to the proposed PRS topology with TE installation (Fig. 1b), the exergy recovery of pressurized NG by TE requires no primary energy input. Hence, TEs can be classified as clean energy resources, similar to PV and wind turbines.
4. The cost of electricity production in the TE-based and traditional microgrids are 0.031 $/kWh and 0.084 $/kWh, respectively. This reduction is due to TEs recovering exergy without consuming primary energy. In the case study, approximately 71% of the electrical demand is supplied by the TE, significantly reducing the operating costs of the TE-based microgrid, as illustrated in Fig. 9.
5. As previously explained, approximately 71% of the electrical demand is supplied by the TE. Also, the combination of ICE and absorption chiller is used as a CCHP system to meet the electrical, cooling, and heating needs of the microgrid. Given these explanations and the high investment cost of the PV array, it is not selected in the simulation outputs in either case.
6. Although the initial capital cost of TEs is higher than that of other energy resources, such as ICEs, this study demonstrates that the overall economic performance of TE-based microgrids is superior due to reduced operating costs.
7. The utilization of the cooling energy from the cold exhaust NG of TEs further enhances the economic benefits of TE-based microgrids. In effect, TEs partially replace absorption and electric chillers, which have higher operating costs. Therefore, similar to electrical energy recovery, the lower operating costs of TEs offset their higher initial capital costs.
8. Globally, numerous city gas stations and town board stations offer potential sites for TE installation. This study demonstrates that incorporating TEs in microgrids

improves their economic performance and maximizes the utility of the TE equipment.

9. The primary function of TEs is to reduce pressure, and they are designed based on the required NG pressure and flow rate in the local distribution network. Consequently, microgrid designers cannot directly control the nominal size or output power of TEs. This characteristic is similar to other non-dispatchable energy resources, such as PV and wind turbines. However, unlike PV and wind turbines, the nominal size of a TE cannot be adjusted to meet specific microgrid energy demands. Therefore, using TEs as an energy resource within microgrids, rather than as conventional DG units, represents a more effective approach, as demonstrated in this study.
10. The issue of controlling the frequency and voltage of a microgrid based on TE, taking into account the unique characteristics of TE and the design and development of a pilot model of this type of microgrid, is one of the proposals that can be carried out in future studies.

VII. Conclusion

In PRSs, replacing traditional pressure regulators with TEs allows the mechanical exergy of NG, which is otherwise wasted as heat, to be harnessed for electricity generation. The expansion process in TEs results in a significantly greater temperature drop compared to pressure regulators, producing substantial cooling energy in the outlet NG. This cooling energy can be recovered through a heat exchanger to satisfy cooling demands. This study introduces, for the first time, the concept of integrating a TE within a microgrid to simultaneously meet its cooling, heating, and electricity demands. The proposed microgrid consists of a TE, ICE, BB, PV system, AB, HST, AC, and EC. A novel multi-objective optimization algorithm is developed to determine the optimal type and size of the energy generation and storage systems, with the objective of minimizing annualized initial capital and O&M costs.

An economic assessment of the proposed microgrid, both with and without the TE, is performed using multiple evaluation methods, including NPV, IRR, and PP. The comparison demonstrates that the TE-based microgrid achieves superior economic performance and lower emissions compared to the traditional microgrid without a TE. Therefore, the integration of TEs in microgrids is strongly recommended.

References

[1] http://unfccc.int/paris_agreement/items/9485.php

[2] Kostowski, W.: 'The possibility of energy generation within the conventional natural gas transport system', *Strojarstvo*, 2010, 52, (4), pp. 429-440.

[3] Poživil, J.: 'Use of expansion turbines in natural gas pressure reduction stations', *Acta Montanistica Slovaca*, 2004, 9, pp. 258-260.

[4] Darabi, A., Shariati, A., Ghanaei, R., Soleimani, A.: 'Economic assessment of a hybrid turboexpander-fuel cell gas energy extraction plant', *Turkish Journal of Electrical Engineering & Computer Sciences*, 2016, 24, pp. 733-745.

[5] Maddaloni, J.D., Rowe, A.M.: 'Natural gas energy recovery powering distributed hydrogen production', *International Journal of Hydrogen Energy*, 2007, 32, pp. 557-566.

[6] Alilou, M., Younesi, A., Sinao, P.: 'A sustainable approach to hybrid microgrid design: Optimal sizing and energy management', *Renewable Energy*, 2026, 256, pp. 1-13.

[7] Atef, M., Alahakoon, S., Wolfs, P., Mumtahina, U.: 'Energy Management in Microgrids: Commercial, Industrial, and Residential Perspectivese', *energies*, 2026, 19, (419), pp. 1-28.

[8] Lejia, L.: 'Optimizing microgrid energy management with hybrid energy storage systems using reinforcement learning methods', *Sustainable Computing: Informatics and Systems*, 2025, 47, pp. 726-749.

[9] Riaz, M., Ahmad, S., Naeem, M.: 'Energy Management of Cooperative Combined Cooling, Heating, and Power Microgrids Considering User Comfort', *IEEE access*, 2025, 13, pp. 76963-76980.

[10] Li, M., Mu, H., Li, N., Ma, B.: 'Optimal design and operation strategy for integrated evaluation of CCHP (combined cooling heating and power) system', *Energy*, 2016, 99, pp. 202-220.

[11] Li, M., Li, H., Zhai, X.: 'Study of a solar-wind-hydrogen-gas-grid multi-energy system with CCHP distributed cooperative operation, *Applied Thermal Engineering*, 2025, 280, pp. 556-571.

[12] Bloch, H.P., Soares, C.: 'Turboexpanders and process applications', (Gulf Professional Publishing, Houston, 2001, 1st edn.)

[13] Howard, C., Oosthuizen, P., Peppley, B.: 'An investigation of the performance of a hybrid turboexpander-fuel cell system for power recovery at natural gas pressure reduction stations', *Chemical Engineering Transaction*, 2010, 21, pp. 37-42.

[14] Ghanaee, R., Akbari Foroud, A.: 'Economic analysis and optimal capacity sizing of turbo-expander based microgrid', *IET Renewable power generation*, 2016, 11, pp. 511-520.

[15] Rahman, M.M.: 'Power generation from pressure reduction in the natural gas supply chain in Bangladesh', *Journal of Mechanical Engineering*, 2010, 41, pp. 89-95.

[16] Anonto, H., Hossain, M., Shufian, A., et al.: 'Intelligent energy management of microgrids using machine learning: Leveraging random forest models for solar and wind power', *Results in Engineering*, 2025, 27, 636-651.

[17] Palma, R., Benavides, C., Lanas, F., Reyes, L., Llanos, J., Saez, D.: 'A microgrid energy management system based on the rolling horizon strategy', *IEEE Transactions on Smart Grid*, 2013, 2, pp. 996-1006.

[18] Mahmoud, M.S., Rahman, M.S., Alsunni, F.M.: 'Review of microgrid architectures - a system of systems perspective', *IET Renewable Power Generation*, 2015, 9, (8), pp. 1064-1078.

[19] Al-Sulaiman, F., Hamdullahpur, F., Dincer, I.: 'Performance comparison of three trigeneration systems using organic', Energy, 2011, 36, pp. 5741-5754.

[20] Sheikhi, A., Ranjbar, A.M., Oraee, H.: 'Financial analysis and optimal size and operation for a multicarrier energy system', Energy and Buildings, 2012, 48, pp. 71-78.

[21] Wei, D., Chen, A., Sun, B., Zhang, C.: 'Multi-objective optimal operation and energy coupling analysis of combined cooling and heating system', *Energy*, 2016, 98, pp. 296-307.

[22] Elmer, T., Worall, M., Wu, S., Riffat, S.B.: 'Emission and economic performance assessment of a solid oxide fuel cell micro-combined heat and power system in a domestic building', *Applied thermal engineering*, 2015, 90, pp. 1082-1089.

[23] Basu, A.K.: 'Microgrids planning of fuel energy management by strategic deployment of CHP-based DERs – an evolutionary algorithm approach', *Electrical Power and Energy Systems*, 2013, 44, pp. 326-336.

[24] Hedman, B.: 'Waste Energy Recovery Opportunities for Interstate Natural Gas Pipelines', Interstate natural gas association of America, 2008.

Biographies